71st Annual Congress
ISSN 1516-392X

INFLUENCE OF STRAIN RATE ON THE FUNCTIONAL BEHAVIOR OF A NITI ALLOY UNDER PSEUDOELASTIC TRAINING*

Mariana Carla Mendes Rodrigues[1]
Guilherme Corrêa Soares[2]
Vicente Tadeu Lopes Buono[3]
Leandro de Arruda Santos[4]

Abstract
The present study deals with the effects of strain rate on the functional behavior of NiTi thin wires. The samples, in the austenitic condition at room temperature, were mechanically cycled 20 times by loading up to 6% strain followed by complete unloading, at 25°C. Four different quasi-static strain rates were assessed: $1x10^{-4}$, $1x10^{-3}$, $1x10^{-2}$ and $5x10^{-2}s^{-1}$. The functional properties are described by means of critical stress to induce martensite, stress at maximum strain, energy dissipated per cycle and residual strain. The sensitivity of repeated cyclic deformation to strain rate is also analyzed in terms of phase stability. The results show that the fluctuation in the loading plateau, due to non-homogeneous transformation, increases with increasing strain rate. During cycling, it is observed that higher strain rates result in lower critical stress to induce martensite after the 5th cycle. However, the stress at maximum strain is higher at high strain rates, regardless the number of cycles. The accumulation of residual strain also increases with the strain rate due to the higher applied stress. During unloading, both the elastic deformation of stress-induced martensite and the reverse transformation seem to overlap at high strain rates. The dissipated energy behavior changes between the 1st and 20th cycle. No martensite is stabilized after training, but the intensity of the X-ray diffraction peaks of austenite increases with strain rate, as a result of stress relaxation.
Keywords: NiTi; Training; Cyclic deformation; Strain rate; Functional behavior.

[1] *Bachelor of Science in Materials Engineering, Master's student, Department of Metallurgical and Materials Engineering, UFMG, Belo Horizonte, MG, Brazil.*
[2] *Bachelor of Science in Metallurgical Engineering, Master's student, Department of Metallurgical and Materials Engineering, UFMG, Belo Horizonte, MG, Brazil.*
[3] *Doctor, Professor, Department of Metallurgical and Materials Engineering, UFMG, Belo Horizonte, MG, Brazil.*
[4] *Doctor, Professor, Department of Metallurgical and Materials Engineering, UFMG, Belo Horizonte, MG, Brazil.*

** Technical contribution to the 71º Congresso Anual da ABM – Internacional and to the 16º ENEMET - Encontro Nacional de Estudantes de Engenharia Metalúrgica, de Materiais e de Minas, part of the ABM Week, September 26th-30th, 2016, Rio de Janeiro, RJ, Brazil.*

1 INTRODUCTION

Shape memory alloys (SMAs) have intrinsic characteristics by exhibiting shape memory effect (SME) and superelasticity (SE). The SME refers to the ability of the material, after experiencing nonlinear pseudoplastic deformation, to recover its original shape upon heating above a critical temperature. On the other hand, the SE, also named as pseudoelasticity (PE), occurs when the material is largely deformed, but spontaneously recovers its shape by the time the applied mechanical load is removed [1-3]. Both phenomena are directly associated with the solid-state martensitic transformation (MT), which is induced by heating (or cooling) or by loading (or unloading), depending on the material's temperature [4].

Amongst the SMAs, NiTi based SMAs are the most favorable materials for most shape memory and superelastic applications nowadays. Besides their best SME and SE properties, NiTi SMAs have other advantages in terms of corrosion resistance, fatigue resistance, ductility, abrasion resistance, biofunctionality and biocompatibility [2,5]. In the midst of their several uses, NiTi SMAs have been employed in several applications in which the device is subjected to mechanical and/or thermal cycling, such as cardiovascular stents, tracheal stents, vena cava filters, thermal actuators, and so on [2,6,7].

The success of those cyclic applications depends on the device's ability to maintain its functional properties stable when in service. Due to this, NiTi SMAs are frequently required to be "trained" before practical use in order to obtain a more stable and well known mechanical behavior [8-10]. This training process consists of carrying out thermal and/or mechanical cycling in the SMA in order to successively induce the formation of martensite and austenite, thus creating a dislocation pattern in the material and a preferable orientation path to the martensite variants [9,11]. As a consequence of training, there is an increase in the resistance of the material towards the formation of further dislocations, then more stable characteristics are achieved [12].

There are many types of training, but since there are a lot of superelastic applications of NiTi SMAs, the study of pseudoelastic training has a considerable importance. Loading and unloading stresses, mechanical hysteresis (dissipated energy), and residual strain are important parameters that characterize the superelastic behavior of a SMA [13]. Moreover, transformation temperatures and phase stability play an essential role in the alloy demeanor [2]. It is well known that all these properties depend directly on cyclic loading, test temperature, loading conditions and strain rate [4,8-10]. Therefore, understanding those properties is very important since they have to be taken into account in the design of SMA elements for practical applications [14,15].

Although there are some previous works dealing with pseudoelastic cycling of NiTi based SMAs under different strain rates [8,15-21], there is still a lack of new studies on this topic and the need to better understand the effect of that variable on phase stability and related functional properties of those materials.

In the present study, the influence of a range of strain rates on the cyclic behavior is investigated by pseudoelastic training of a NiTi SMA in the form of wire. The effects of strain rate on the functional properties, such as critical stress to induce martensite, dissipated energy, residual strain and stress at maximum strain are discussed in detail. The influence of pseudoelastic training at different strain rates on the phase stability is also evaluated.

2 MATERIAL AND METHODS

The material used in this study was a 1.0mm NiTi SMA in the form of wire, provided by Nitinol Devices and Components (Fremont, CA, USA) in a cold rolled and annealed condition. The nominal chemical composition was 51,4at.% Ni and 48,6at.% Ti, as measured by Energy-dispersive X-ray spectroscopy (EDS). Differential scanning calorimetry (DSC), performed in the wire as received, showed that the austenite finish temperature (Af) was -2.3°C, so the material was in the superelastic state at room temperature.

Pseudoelastic cycling tests were done using an Instron 5582 universal testing machine (Instron, Norwood, MA, USA). Wire specimens with a total length of 150mm and gauge length of 90mm were used in the tests. The cycling consisted of loading the specimens up to a 6% strain followed by a complete unloading, down to 0MPa, under a constant temperature of 25°C. For this, four different strain rates, in the quasi-static regime, were assessed: $1x10^{-4}$, $1x10^{-3}$, $1x10^{-2}$ and $5x10^{-2}s^{-1}$. Those values were chosen in order to check quasi-static conditions. A total of twenty pseudoelastic cycles were performed and a new specimen was used in each test.

The behavior of the functional properties, such as critical stress to induce martensite, dissipated energy, cumulative residual strain, and stress at maximum strain, with increasing number of cycles and at each strain rate, was evaluated. Due to constant changes in the hysteresis loop with cycling, measuring the critical stress to induce martensite is not so easy. Thus, for the purpose of this paper, this parameter was assessed by the intersection point of the hysteresis curve and a line parallel to the austenite apparent elastic modulus shifted to 0.2% strain to the right [22,23]. Dissipated energy, cumulative residual strain and stress at maximum strain were calculated as being the area within the hysteresis loop, the accumulation of remnant strain after unloading to 0MPa, and the stress at 6% strain, respectively. In order to avoid possible manipulation errors, all those parameters were measured and extracted directly from the Bluehill 2 software.

Moreover, the effect of different strain rates on pseudoelastic training was checked in terms of phase stability. Since the mechanical features of martensite and austenite varies significantly from each other, knowing that variable is essential for the success of the device. Phase stability was investigated by X-ray diffraction (XRD) using a PANanalytical PW1710 (Almelo, The Netherlands) diffractometer with Cu-Kα radiation (λ=1.54060 Å) at room temperature. The parameters used for the measurements were as follows: 35kV voltage; 50mA anode current; scanning angle from 20 to 90°2θ; step size of 0.02°2θ and exposure time of 2.5 seconds per step. Crystalline plans were indexed based on standard X-ray diffraction patterns obtained from the Inorganic Crystal Structure Database (ICSD) [24].

3 RESULTS AND DISCUSSION

Figure 1 shows the stress-strain curves of 20 cycles for each strain rate evaluated. As can be seen, the alloy presents distinct mechanical hysteresis in response to different strain rates, which means that variation on strain rate may promote considerable changes in the alloy functional properties.

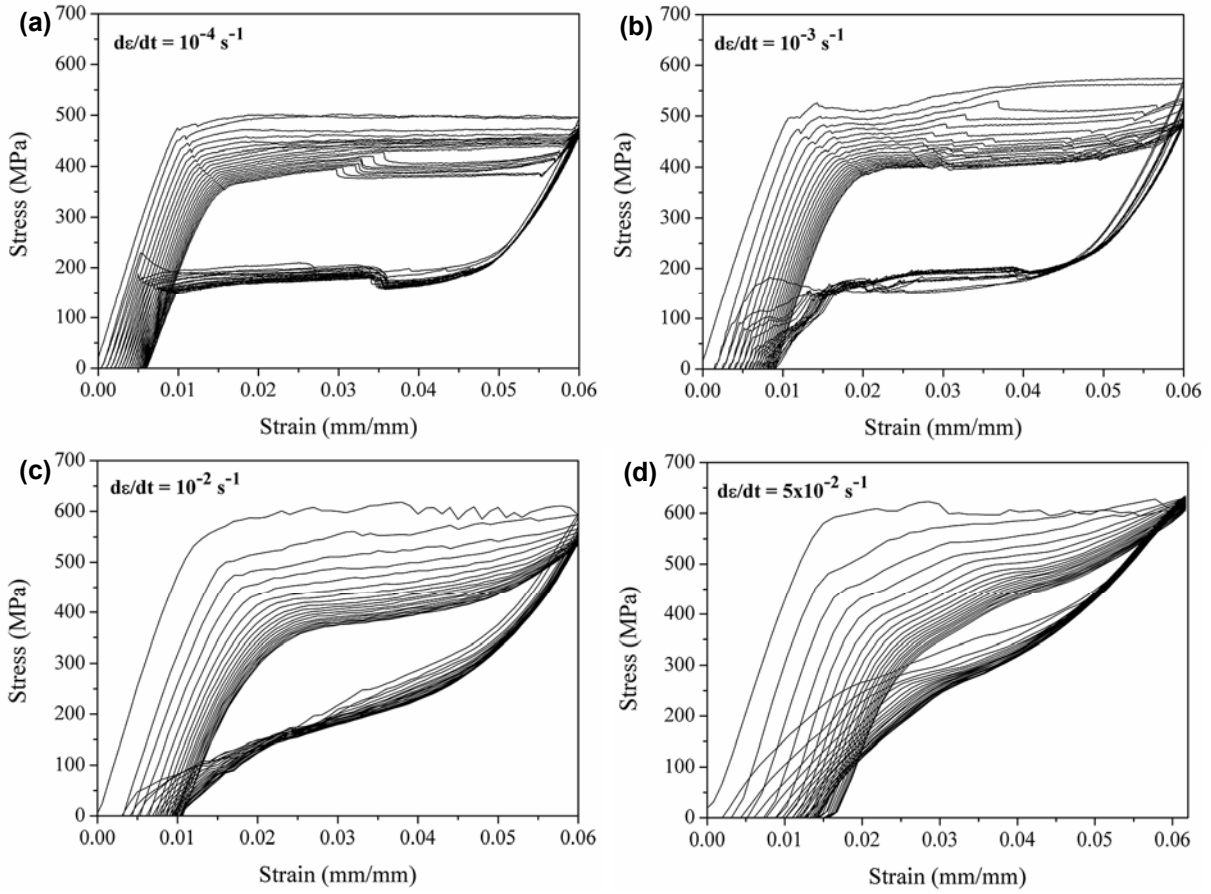

Figure 1. Stress-strain curves at strain rates of (a) $10^{-4}s^{-1}$; (b) $10^{-3}s^{-1}$; (c) $10^{-2}s^{-1}$ and (d) $5x10^{-2}s^{-1}$.

It is seen from Figure 1 (c) and (d) that for strain rates of 10^{-2} and $5x10^{-2}s^{-1}$ there are some small fluctuations in the martensitic transformation (MT) plateau in the first cycle. Tobushi et al. [8] also observed this behavior for strain rates ≥ $1.6x10^{-3}s^{-1}$. According to them, at low strain rates, there is enough time for the interfaces between martensite and austenite to move, then a high stress required to move those interfaces is relaxed. Thus, MT occurs more homogeneously and no fluctuation appears. But at high strain rates those interfaces move quite fast and, consequently, there is shorter time for the stress relaxation to occur. Therefore, the internal frictional resistance against the movement of the interfaces is increased, resulting in a higher fluctuation level. However, during cycling, the resistance force that impedes the progress of MT diminishes due to increased internal stresses, and therefore, no more significant fluctuations are observed at further cycles, as can be verified in Figures 1 (c) and (d). Figure 1 (a) indicates that only at lower strain rates, such as one of $10^{-4}s^{-1}$, the plateaus associated with MT and reverse transformation (RT) occur at relatively constant stresses. This can be explained by the fact that due to the lower strain rate, most of the heat generated/absorbed during the phase transformations is exchanged with the environment. However, at higher strain rates, there is not enough time for the temperature to keep constant, then a self-heating/cooling of the specimen may take place due to latent heat [2,4]. This result is consistent with the one verified by McCormick et al. [16]. It is remarkable how the RT plateau becomes more leaned as strain rate increases [14-16,18,19], as can be seen by comparing this behavior amongst all the strain rates in Figure 1. So it seems reasonable to assume that the

segments regarding the elastic unloading of the stress-induced martensite (SIM) and the RT tend to overlap in the extent that strain rate increases [18].
Figure 2 (a), (b) and (c) illustrate how strain rate influences the critical stress to induce martensite, the stress at maximum strain and the residual strain, respectively.

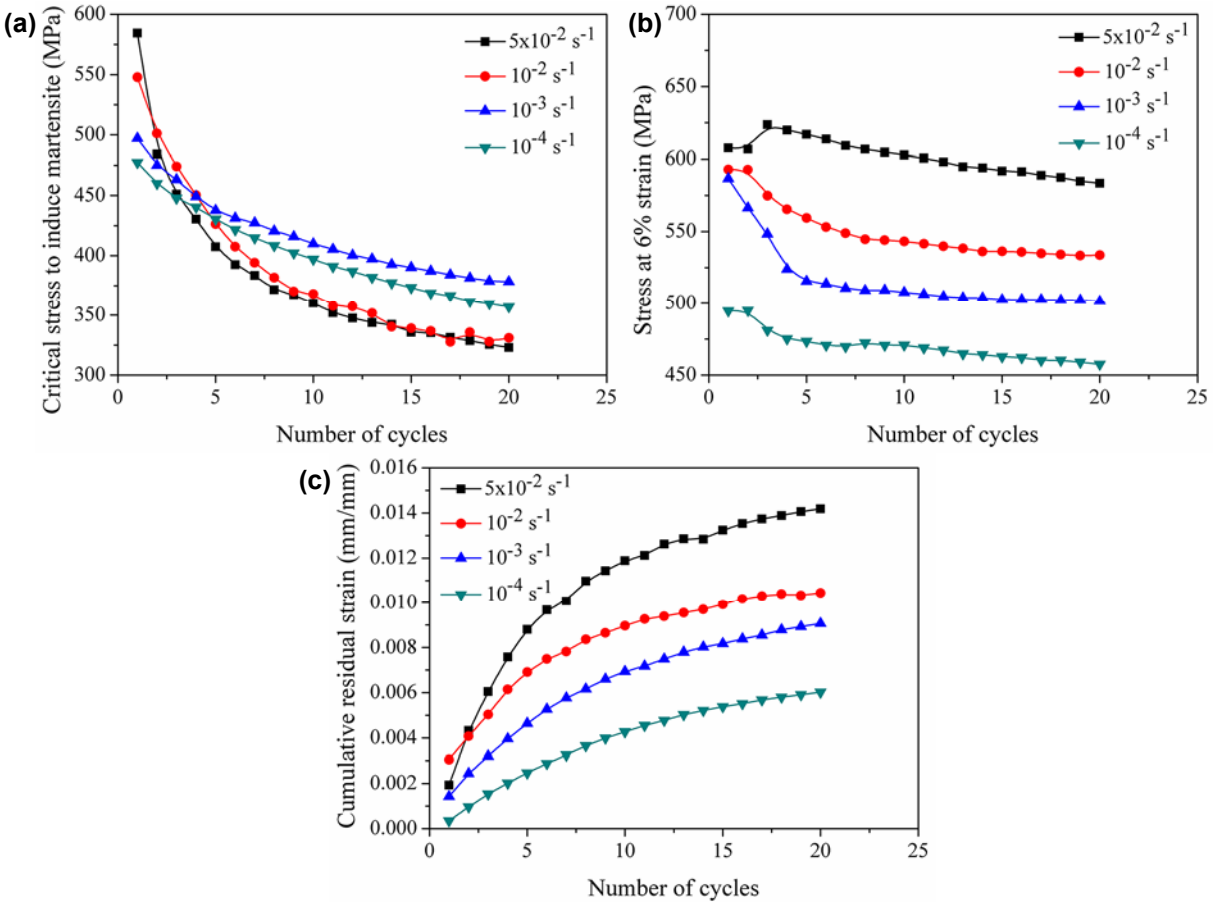

Figure 2. Influence of strain rate on (a) critical stress to induce martensite; (b) stress at maximum strain and (c) cumulative residual strain.

From Figure 2 (a) one can see that, considering the first cycle, the critical stress to induce martensite increases with strain rate [18]. This happens because the MT is a termomechanical transformation, which means that the increase in the specimen's temperature during the test, as a result of its self-heating during MT, stabilizes the austenitic phase, consequently requiring a higher stress to induce martensite [19]. To Tobushi and co-workers [8], that behavior was only observed at strain rates $> 3.3x10^{-4}s^{-1}$. They stated that the critical stress to induce martensite does not depend on strain rate when it is $\leq 3.3x10^{-4}s^{-1}$.
The reduction of the critical stress to induce martensite with increasing the number of cycles occurs in a more pronounced way when it comes to higher strain rates [17]. As a consequence, after a few cycles, the critical stress to induce martensite at $5x10^{-2}$ and $10^{-2}s^{-1}$ becomes lower than at 10^{-3} and $10^{-4}s^{-1}$ (Figure 2 (b)). Due to the higher stress required to the first formation of SIM at higher strain rates, slip deformations occur more easily. Such deformations create internal stresses in the material's microstructure, which assist the occurrence of MT, thus resulting in a lower applied stress to induce martensite in the further cycles [17]. Figure 2 (b) shows that the behavior of the stress at maximum strain differs from the critical stress to induce

martensite, shown in Figure 2 (a). From Figure 2 (b), one can see that the higher the strain rate, the higher is the stress at maximum strain, regardless the number of cycles. It is also noticed that the most significant change in that stress occurs up to 5 cycles in all strain rates, from when the stress at maximum strain tends to assume a more stable behavior.

Figure 2 (c) shows that cumulative residual strain increases more significantly with increasing strain rate. The same result was ascertained by Tobushi et al. [8], Strnadel et al. [17] and Dayananda and Rao [18]. It is clearly shown on that figure that the accumulation of residual strain in the first cycle is quite similar for all strain rates [19]. However, the difference on cumulative residual strain amongst all the strain rates increases considerably with number of cycles. Due to the higher stresses required to form SIM at higher strain rates, more dislocations are introduced in the material. These dislocations may allow the generation of residual martensite, because of the stress fields generated in the material's microstructure, and/or contribute to the accumulation of irreversible deformation [25,26]. So it seems reasonable to assume that the cause of residual strain can be both, residual martensite and plastic deformation [21,25,27]. With an increasing number of cycles, the dislocation density becomes more saturated and a more stable behavior is observed.

The dissipated energy, i.e. the mechanical hysteresis, is directly affected by strain rate as shown in Figure 3.

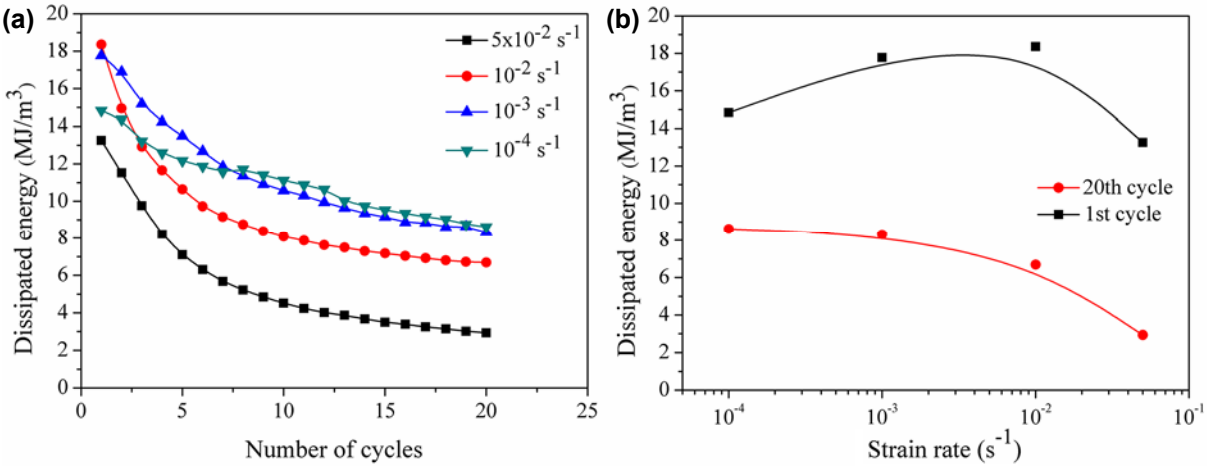

Figure 3. Dissipated energy as a function of (a) number of cycles; (b) strain rate.

It is seen from Figure 3 (a) that the dissipated energy changes more gradually as far as the strain rate diminishes, which was also reported by Desroches et al. [19]. As previously stated, at higher strain rates the RT plateau becomes more inclined (Figure 1). Since such inclination is more pronounced than the upward translation of the MT plateau, this results in a reduction in the hysteresis loop. That is the reason why the dissipated energy at all strain rates tends to reduce at a higher cycle count. From a microscopic point of view, mechanical hysteresis decreases because insofar the martensite is "trained" with cycling, the creation and rearrangement of defects and the friction generated by the movement of martensite variants become lower, and as a consequence, the energy dissipation during MT and RT decreases [7,28].

As can be seen in Figure 3 (b), considering the behavior in the first cycle, the dissipated energy is maximum at strain rates between 10^{-3} and $10^{-2}s^{-1}$, reducing considerably at higher ones. This behavior was also observed by Dayananda and Rao [18] and Zurbitu et al. [20] in a similar range of strain rate. According to those authors, this demeanor

results from changes in the transformation stresses due to variations during RT: while at intermediate rates (10^{-3} and $10^{-2}s^{-1}$) the RT temperature decreases (also reducing the reverse transformation stress), at higher strain rates that temperature increases, thus increasing the reverse transformation stress and, therefore decreasing the energy dissipated. That behavior seems to change under temperature controlled conditions [15]. A different behavior was also verified by Tobushi et al. [8] who found that the dissipated energy does not depend on strain rate when it is ≤ $3.3x10^{-4}s^{-1}$, although that energy increases with increasing strain rate when it is ≥ $1.6x10^{-3}s^{-1}$. On the other hand, as shown in Figure 3 (b), after performing 20 cycles, there is a continuous decrease of the dissipated energy when increasing strain rate. As far as cycling goes on, the self-heating of the specimen due to release of latent heat is still significant, which results in a decrease in the dissipated energy, as compared with the behavior after the 1st cycle, irrespective of the strain rate.

Figure 4 shows the XRD patterns of the as received NiTi sample, as well as of the samples after being pseudoelastically trained at different strain rates.

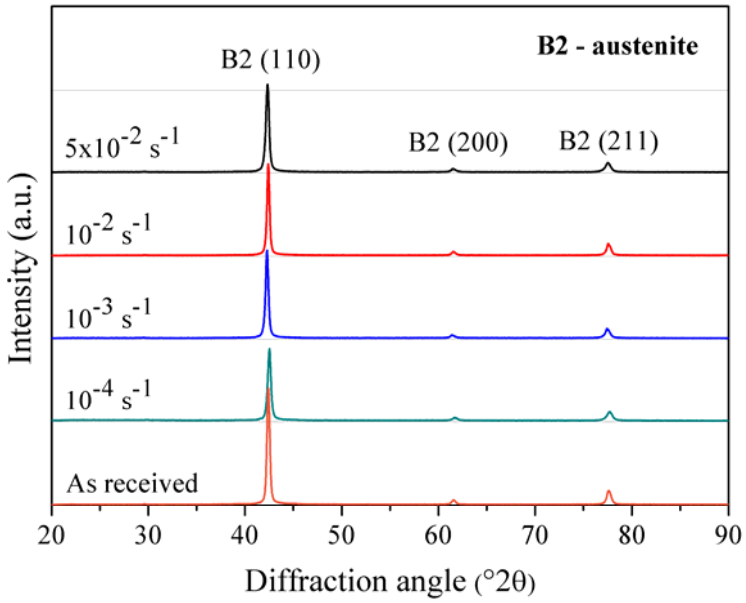

Figure 4. XRD patterns of NiTi samples before and after training at different strain rates.

One can see from Figure 4 that, in comparison with the as received sample, the intensity of the main austenite peak decreases for all strain rates studied, which is certainly related to the introduction of defects with cycling. However, peak intensity increases to the extent that the strain rate also increases. It seems reasonable to assume that higher strain rates result in a more prominent increase in the specimen's temperature, which somehow causes relaxation on the internal stresses promoted by cycling and increases the austenite stability. This explains the increase in the peaks intensity with an increase in strain rate and is in agreement with Brinson and co-workers [21], who claimed that the magnitude of the stress relaxation decreases with decreasing strain rate. Nevertheless, further microstructural analyzes, such as transmission electron microscopy have to be done to confirm that explanation. It is also noticed from Figure 4 that no peak related to the martensitic phase was detected by the XRD analyzes, which suggests that either the number of cycles or the strain amplitude used in the training were not enough to stabilize martensite [14,29,30].

4 CONCLUSIONS

The present study focuses on the behavior of functional properties and its strain rate dependence during pseudoelastic training in a NiTi SMA wire. The results obtained can be summarized as follows.

(1) Strain rate was shown to have a strong influence on the superelastic behavior of the NiTi alloy analyzed. Taking into account the 1st cycle, higher strain rates increased the critical stress to induce martensite because of the specimen's temperature increase, due to the latent heat of transformation, which cannot be totally dissipated in the case of high strain rates. However, higher critical stress to induce martensite induces more dislocation density in the microstructure, which causes larger decrements in the critical stress to induce martensite during cycling. So, after the 5th cycle, the higher the strain rate the lower is the critical stress to induce martensite.

(2) High strain rates lead to the appearance of fluctuations in the martensitic transformation plateau, due to the fact that at those rates the interfaces between parent (austenite) and martensite move faster and therefore there is just a short time to relax the stress between the interfaces. Thereby, the internal friction resistance against the interface movements increases, which results in a heterogeneous transformation.

(3) In the case of lower strain rates, stress plateaus regarding martensitic and reverse transformations are well defined in all 20 cycles. However, in the case of higher strain rates, slopes of the stress-strain curves get steeper in the phase transformation regions as the number of cycles increases. This suggests that at those strain rates, the austenite formation and the elastic deformation of stress-induced martensite occur simultaneously.

(4) The dissipated energy behavior at each strain rate exhibited substantial difference between the 1st and the 20th cycles. In the 1st cycle, strain rates of $10^{-3}s^{-1}$ e $10^{-2}s^{-1}$ caused higher dissipated energy, however, in the 20th cycle, this energy decreased with increasing strain rate.

(5) Cumulative residual strain increased with number of cycles and with strain rate, which is directly related to the introduction of defects during cycling and to the higher imposed stress to induce martensite, respectively. However, the residual strain per cycle diminishes further as the number of cycles increases.

(6) In the XRD analyzes no peak related to the martensitic phase was identified for any strain rate investigated. This suggests that the conditions used in the cycling were not enough to stabilize martensite. On the other hand, the intensity of the austenite peaks increased as far as strain rate increased. This probably happened because higher strain rates promote an increase in the internal temperature of the specimen during cycling. As a consequence, more stress relaxation can occur in the material and the austenitic phase can become more stable.

(7) Strain rate showed to be a really important parameter to be taken into account in the design of SMA elements.

Acknowledgments

The authors gratefully acknowledge support from Coordenação de Aperfeiçoamento de Pessoal de Nível Superior (CAPES), Pró-Reitoria de Extensão da Universidade Federal de Minas Gerais (PROEX-UFMG), Conselho Nacional de Desenvolvimento

Científico e Tecnológico (CNPq) and Fundação de Amparo à Pesquisa do Estado de Minas Gerais (FAPEMIG).

REFERENCES

1 Otsuka, K.; Shimidzu, K. Pseudoelasticity and shape memory effects in alloys. International Metals Reviews. 1986; 31(3): 93-114.
2 Otsuka, K.; Wayman, C. M. Shape memory materials. New York: Cambridge, 1998.
3 Otsuka, K.; Ren, X. Physical metallurgy of Ti-Ni-based shape memory alloys. Progress in Materials Science. 2005; 50(5): 511-678.
4 Shaw, J. A.; Kyriakides, S. Thermomechanical aspects of NiTi. Journal of Mechanics and Physics of Solids. 1995; 43(8):1243-1281.
5 Shaw, J. A.; Churchill, C. B.; Ladicola, M. A. Tips and tricks for characterizing shape memory alloy wire: Part I-Differential scanning calorimetry and basic phenomena. Experimental Techniques. 2008; 32: 55-62.
6 Simon, M.; Kaplow, R.; Salzman, E.; Freiman, D. A vena cava filter using thermal shape memory alloy experimental aspects. Radiology. 1977; 125:89-94.
7 Duerig, T. W.; Melton, K. N.; Stöckel, D.; Wayman, C. M. Engineering Aspects of Shape Memory Alloys. Great Britain: Butterworth-Heinemann Ltd, 1990.
8 Tobushi, H.; Shimeno, Y.; Hachisuka, T.; Tanaka, K. Influence of strain rate on superelastic properties of TiNi shape memory alloy. Mechanics of Materials. 1998; 30: 141-150.
9 Miyazaki, S.; Imai, T; Igo, I; Otsuka, K. Effect of cyclic deformation on the pseudoelasticity characteristics of Ti-Ni alloys. Metallurgical Transactions A. 1986, 17: 115-120.
10 Tang, W.; Sandström, R. Analysis of the influence of cycling on TiNi shape memory alloys properties. Materials & Design. 1993; 14(2): 103-113.
11 Miller, D. A.; Lagoudas, D. C. Influence of cold work and heat treatment on the shape memory effect and plastic strain development of NiTi. Materials Science and Engineering A. 2001; 308: 161-175.
12 Contardo, L.; Guénin, G. Training and two way memory effect in Cu-Zn-Al alloy. Acta Metallurgica et Materialia. 1990; 38(7): 1267-1272.
13 Shahmir, H.; Nili-Ahmadabadi, M.; Naghdi, F. Superelastic behavior or aged and thermomechanical treated NiTi alloy at Af +10°C. Materials and Design. 2011; 32: 365-370.
14 Takeda, K.; Tobushi, H.; Miyamoto, K.; Pieczyska, E. A. Superelastic deformation of TiNi shape memory alloy subjected to various subloop loadings. Materials Transactions. 2012; 53(1): 217-223.
15 Pieckzyska, E.; Gadaj, S.; Nowacki, W. K.; Hoshio, K.; Makino, Y.; Tobushi, H. Characteristics of energy storage and dissipation in TiNi shape memory alloy. Science and Technology of Advanced Materials. 2005; 6: 889-894.
16 McCormick, P. G.; Liu, Y. Intrinsic thermal-mechanical behaviour associated with the stress induced martensitic transformation in NiTi. Materials Science and Engineering. 1993; 167: 51-56.
17 Strnadel, B.; Ohashi, S.; Ohtsuka, H.; Miyazaki, S.; Ishihara, T. Effect of mechanical cycling on the pseudoelasticity characteristics of Ti-Ni and Ti-Ni-Cu alloys. Materials Science and Engineering A. 1995; 203: 187-196.
18 Dayananda, G. N.; Rao, M. S. Effect of strain rate on properties of superelastic NiTi thin wires. Materials Science and Engineering A. 2008; 486: 96-103.
19 Desroches, R.; McCormick, J.; Delemont, M. Cyclic properties of superelastic shape memory alloy wires and bars. Journal of Structural Engineering. 2004; 130(1): 38-46.
20 Zurbitu, J.; Santamarta, R.; Picornell, C.; Gan, W. M.; Brokmeier, H. G.; Aurrekoetxea, J. Impact fatigue behavior of superelastic NiTi shape memory alloy wires. Materials Science and Engineering A. 2010; 528: 764-769.

21 Brinson, L. C.; Shmidt, I.; Lammering, R. Stress-induced transformation behavior of a polycrystalline NiTi shape memory alloy: micro and macromechanical investigations via in situ optical microscopy. Journal of the Mechanics and Physics of Solids. 2004; 52: 1549-1571.
22 Gall, K.; Tyber, J.; Brice, V.; Frick, C. P.; Maier, H. J.; Morgan, N. Tensile deformation of NiTi wires. Journal of Biomedical Materials Research Part A. 2005; 75(4): 810-823.
23 Lin, B.; Gall, K.; Maier, H. J.; Waldron, R. Structure and thermomechanical behavior of NiTiPt shape memory alloy wires. Acta Biomaterialia. 2009; 5: 257-267.
24 Inorganic Crystal Structure Database (ICSD), FIZ Karsruhe: Gmelin-Institut für anorganische Chemie und Fashionformatszetrum, 2007.
25 Saikrishna, C. N.; Ramaiah, K. V.; Bhaumik, S. K. Effects of thermo-mechanical cycling on the strain response of Ni–Ti–Cu shape memory alloy wire actuator. Materials Science and Engineering A. 2006; 428: 217-224.
26 Yawny, A.; Olbricht, J.; Sade, M.; Eggeler, G. Pseudoelastic cycling and ageing effects at ambient temperature in nanocrystalline Ni-rich NiTi wire. Materials Science and Engineering A. 2008; 481-482: 86-90.
27 Eggeler, G.; Hornbogen, E.; Yawny, A.; Heckmann, A.; Wagner, M. Structural and functional fatigue of NiTi shape memory alloys. Materials Science and Engineering A. 2004; 378: 24-33.
28 Ma, J.; Karaman, I.; Maier, H. J.; Chumlyakov, Y. I. Superelastic cycling and room temperature recovery of $Ti_{74}Nb_{26}$ shape memory alloy. Acta Materialia. 2010; 58: 2216-2224.
29 Delaflor, S.; Urbina, C.; Ferrando, F. Effect of mechanical cycling on stabilizing the transformation behavior of NiTi shape memory alloys. Journal of Alloys and Compounds. 2009; 469: 343-349.
30 Tahara, M.; Kim, H. Y.; Hosoda, H.; Miyazaki, S. Cyclic deformation behavior of a Ti–26 at.% Nb alloy. Acta Materialia. 2009; 57: 2461-2469.